Configurational dependence of elastic modulus of metallic glass

Y. Q. Cheng* and E. Ma†
Department of Materials Science and Engineering, Johns Hopkins University, Baltimore, Maryland 21218, USA
(Received 16 May 2009; published 5 August 2009)

The shear modulus (G) of metallic glass depends sensitively on the internal amorphous structure, in addition to being lower than that of the crystal counterpart. To uncover the origin of this behavior, we have performed extensive atomistic simulations of model alloys with varying internal structures, but all at the same $Cu_{50}Zr_{50}$ composition. We demonstrate that G is sensitively dependent on the correlations of the atomic shear stresses. A systematic comparison of these alloys reveals obvious differences in the correlations of the atomic shear stresses in the medium-to-long range, at length scales beyond ~1.2 nm. This reflects a major difference in these different structural configurations, in terms of the transverse coupling between the local atomic clusters and their surrounding confinement. This coupling is strongly influenced by the degree of structural ordering, leading to the obvious configurational dependence of G. The bulk modulus and the underlying correlations of the atomic pressure, in contrast, are insensitive to the configurational variations.

DOI: 10.1103/PhysRevB.80.064104 PACS number(s): 62.20.de, 61.43.Dq

I. INTRODUCTION

The elastic modulus is a fundamental material property, determined by not only the chemistry of the alloy but also its atomic-level configuration. For the emerging bulk metallic glasses (MGs),[1,2] the shear modulus (G) is usually sensitive to the processing history, e.g., the cooling rate, the annealing/aging, and thermal/mechanical rejuvenation.[3–6] In other words, the magnitude of G depends on how the glass is prepared, and the resulting internal structure. The change of bulk modulus (B), in contrast, is usually minor and appears to be a simple density effect.[3,4] The G/B ratio, as a result, is a dimensionless indicator of the internal atomic structure, and is being considered as an important parameter related to material properties such as plasticity.[2] There is thus a pressing need to understand why G is sensitive to the internal atomic-level structures, and how this influences the material's mechanical properties.

The variation of G for MGs with different processing history has been attributed to visitations of different megabasins in the potential energy landscape (PEL) (Refs. 7–9); i.e., for a specific MG, the lower the configurational potential energy, the higher the energy barrier between the megabasins, and correspondingly the larger the G.[3,4,7–9] Alternatively, Granato *et al.* applied an interstitialcy model to MGs.[10–12] By analogy to the dumbbell-like defects in crystals, they proposed that the changing G with relaxation in MGs can be modeled by the evolution of interstitialcy-like defects. In addition, it has been observed that the G of MGs is usually much lower (up to ~30%) than the corresponding crystal at the same composition.[13] According to Weaire *et al.*,[14] the obvious reduction in G from crystal to glass is due to the internal relaxation to a nonaffine strain field that lowers the energy/stress in the amorphous system.[15,16]

In this paper, by studying the atomic stress[17] and its correlation over various length scales, we propose a different microscopic mechanism underlying the general configurational dependence of G. The behavior of G is also compared with that of B, and their contrasting behaviors are explained.

II. MODEL SYSTEMS AND CALCULATION OF ELASTIC MODULUS

Our modeling employs molecular dynamics (MD) simulations,[18] and the embedded-atom-method (EAM) interatomic potentials developed based on first-principle calculations.[19–21] We compare $Cu_{50}Zr_{50}$ MGs obtained with different cooling rates (and the corresponding B2 CuZr crystal as a reference[22]). The $Cu_{50}Zr_{50}$ MGs were obtained by quenching of equilibrium liquid from 2000 to 300 K (NPT ensemble: constant number of particles, pressure, and temperature) at cooling rates of 10^{10}, 10^{11}, and 10^{12} K/s, respectively, with all samples barostated at zero pressure under three-dimensional periodic boundary conditions. For convenience of discussion, MGs obtained using slower cooling rate (or those have experienced annealing/aging), are termed "older" glasses; while those obtained using faster cooling rate (or those have been thermally/mechanically rejuvenated), are termed "younger" glasses. Such a description is meant to differentiate the varying configurational states of the MG (e.g., relaxed versus fresher internal structures). The B2 CuZr was constructed and equilibrated at 300 K and zero pressure. Each sample contains 16 000 atoms (~6.5 nm box size), and the density of the CuZr crystal is found to be ~1% higher than the simulated MGs at 300 K.

Isothermal stiffness coefficients (C) at 300 K were calculated following the fluctuation method.[4,23] For a canonical (NVT: constant number of particles, volume, and temperature) ensemble, C can be decomposed into three contributing terms:

$$^{T}C_{mnpq} = C^{I}_{mnpq} + C^{II}_{mnpq} + C^{III}_{mnpq},$$

where

$$C^{I}_{mnpq} = -\frac{V}{k_B T}(\langle P_{mn}P_{pq}\rangle - \langle P_{mn}\rangle\langle P_{pq}\rangle),$$

$$C^{II}_{mnpq} = \frac{2Nk_BT}{V}(\delta_{mp}\delta_{nq} + \delta_{mq}\delta_{np}),$$

and

$$C^{III}_{mnpq} = \langle \chi_{mnpq} \rangle.$$

$\langle\ \rangle$ denotes the ensemble average. C^{I}_{mnpq} is thus the fluctuation term of stress tensor P; C^{II}_{mnpq} accounts for the contribution from kinetic energy, and C^{III}_{mnpq} is the Born term.[4,23] For a complete derivation of the above equations and detailed expression of each term in the EAM formalism, see Ref. 24.

MD simulations of the NVT ensemble are then employed to sample the configurational space (100 000 time steps, each of 2 fs), until the calculated stiffness coefficients converge. G and B are then obtained from the stiffness coefficients using standard equations for either isotropic materials (MGs) or cubic crystals (B2 CuZr).[24]

III. DECOMPOSED SHEAR MODULUS AND THE PHYSICAL INTERPRETATION

We first discuss G at length to explain its strong configurational dependence. The weak dependence of B will be seen as an accompanying conclusion, borne out of the same analysis.

Corresponding to C^I, C^{II}, and C^{III}, the calculated G is the sum of G^I, G^{II}, and G^{III}. These three contributing terms are not an arbitrary division of the total G, but have separate physical meanings. Thermodynamically, shear modulus can be defined as the second derivative of free energy with respect to shear strain. For an NVT ensemble, the Helmholtz free energy (F) is the sum of kinetic energy, potential energy, and an entropy term ($-TS$). By inspecting the detailed derivation in Ref. 24, it can be found that G^I is essentially the entropic contribution, which corresponds to the second derivative of the entropy term in the free energy, while G^{II} and G^{III} corresponds to the second derivative of the kinetic energy and potential energy (all with respect to shear strain).

The decomposed shear modulus can also be explained in the PEL (Refs. 7–9 and 25) picture. In the (quasi-)equilibrium sampling process, the simulated system is traveling in the PEL following the NVT partitioning.[4,23,24] The calculated G^I actually measures the *fluctuation* of instantaneous *slope* of the sampled potential energy surface, while G^{III} is the *average* of the instantaneous *curvature* (both along the shear direction). The G^{II} term is usually small and negligible for the low temperature range of interest (see below).

The above two interpretations of the decomposed shear modulus are consistent. For example, the fluctuation often means uncertainty, which is usually represented by entropy in thermodynamics.

IV. STRONG CONFIGURATIONAL DEPENDENCE OF SHEAR MODULUS: RUGGEDNESS OF PEL AND ENTROPIC EFFECT

Figure 1 shows the decomposed G terms for the three MGs and the B2 crystal. First of all, we observe that G^{II} is indeed negligibly small at low T. Second, the G^{III} data points of all samples appear to fall nearly on a straight line, indicating that the Born term is almost following a unified (i.e., not configurational sensitive), weak and linear T dependence, which can be reasonably attributed to the thermal expansion (density effect) of the PEL. Third, unlike G^{II} and G^{III}, G^I behaves very differently in the crystal and the various glasses. We thus identify G^I as the key to understand the strong configurational dependence of G.

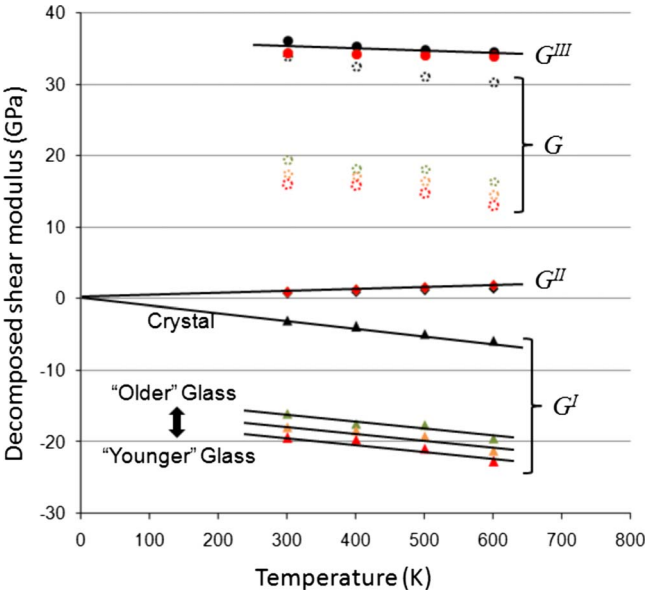

FIG. 1. (Color online) Decomposed shear modulus and their temperature dependence, for $Cu_{50}Zr_{50}$ MGs prepared under three different cooling rates and B2 CuZr crystal. The G (dotted circles) is the sum of G^I (triangles), G^{II} (diamonds), and G^{III} (solid circles). Green, orange, and red colors label MGs cooled at 10^{10}, 10^{11}, and 10^{12} K/s, respectively (from older to younger glass in the figure), with black color for B2 CuZr. G^{II} and G^{III} appear to have a unified linear dependence on T and the data points for different samples almost overlap, while G^I dominates the difference between MGs with different cooling rates (and crystal). Black lines serve as a guide to the eyes.

Then how do we understand the above results, in terms of the physical meaning of the decomposed shear modulus discussed in Sec. III? First of all, the local PEL of the three MGs and the crystal could be very different, as schematically shown in Fig. 2. During the NVT sampling of the PEL, the crystal configuration simply vibrates around the global minimum, while the glass configuration (which is trapped in a megabasin[26]) can still hop between sub-basins (Fig. 2). These sub-basins have very small barriers between them, which is originated from the amorphous nature (i.e., lack of long-range periodicity to coordinate the PEL) of the MGs. In other words, the PEL of MGs is intrinsically rugged and hierarchical.[5,26] The visitation of different sub-basins can be confirmed in simulations. By solving the inherent structure (direct energy minimization) during sampling, the crystal always converges to the global minimum (perfect crystal lattice), while the glass does not converge to a consistent minimum. Instead, the inherent structure of MG is changing/drifting slightly with time, indicating the hopping between sub-basins in the PEL. In real space, the hopping events are observed to correspond to subtle rearrangement of the atomic clusters. Therefore, in the PEL picture, G^{III} (average curvature) can be perceived as an indicator of the average local sub-basin profile, while G^I (slop fluctuation) describes how the sub-basins are organized in the megabasin (Fig. 2). These

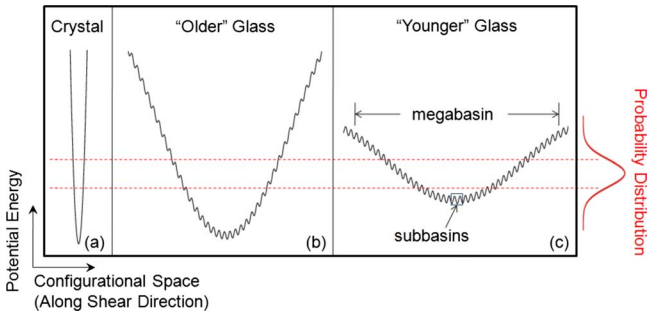

FIG. 2. (Color online) A schematic comparing the local PEL of crystal and different glasses. The probability distribution (schematic only) defines a window (dashed lines) for the most likely sampled regions in the PEL, at the given temperature. For the younger glass, the PEL is flatter in the megabasin, thus the sampled region contains more sub-basins and is more rugged (subject to larger fluctuation/uncertainty). In the perfect crystal, no sub-basin hopping is possible, thus there is only minimum fluctuation due to vibration.

two together determine the overall profile of the megabasin (e.g., the ruggedness, the effective curvature, the barrier height, etc.). In other words, G^{III} is more about "how each sub-basin looks like, on average." and it is not very sensitive to "how they are arranged." G^I, on the other hand, cares about not only the profile of the sub-basin, but more importantly, also "their arrangement." The latter determines the fluctuation (or uncertainty) of the sampled PEL at the given temperature. Specifically, for a crystal, the deep, single (sub-)basin leads to minimum uncertainty. For a glass, however, multiple sub-basins can be sampled with considerable probability (Fig. 2). The higher the cooling rate, the shallower/flatter the local megabasin, thus the more sub-basins are involved, which naturally leads to higher fluctuation/uncertainty.

Thermodynamically, the fluctuation or uncertainty in a crystal corresponds to the vibrational entropy. While in a glass, extra contribution from the sub-basin hopping is important, giving rise to the configurational entropy: the higher the cooling rate (or the younger the glass), the larger the configurational entropy, and the larger the entropic contribution (more negative G^I), thus the smaller the G (see discussion in Sec. V below). In other words, it is the entropic effect that dominates the configurational dependence of G, and the different configurational entropy in MGs is responsible for the different G.

V. STRONG CONFIGURATIONAL DEPENDENCE OF SHEAR MODULUS: MICROSCOPIC ORIGIN

The next step is to understand what is happening at the atomic level that changes the G^I. For isotropic MGs, G^I is essentially C^I_{44} (or C^I_{55}, C^I_{66}, in simulation we average C^I_{44}, C^I_{55}, and C^I_{66} to reduce statistical error[24]). For B2 CuZr, C^I_{44} dominates G^I, and the results are also presented for comparison. For clarity, in the following we illustrate our point using C^I_{44} and P_{xy}, and the complete version used for actual calculation can be found in Ref. 24

$$C^I_{44} = -\frac{V}{k_B T}(\langle P_{xy}P_{xy}\rangle - \langle P_{xy}\rangle\langle P_{xy}\rangle) = -\frac{V}{k_B T}\mathrm{var}(P_{xy}), \quad (1)$$

where $\mathrm{var}(P_{xy})$ is the variance of the shear stress over the sampling time. The stress P_{xy} can be expressed using atomic stresses,

$$P_{xy} = \frac{1}{V}\sum_{i=1}^{N}(m_i v_{i,x}v_{i,y} + r_{i,x}f_{i,y}) = \frac{1}{N}\sum_{i=1}^{N}\frac{m_i v_{i,x}v_{i,y} + r_{i,x}f_{i,y}}{\bar{V}} = \frac{1}{N}\sum_{i=1}^{N} p_{i,xy}, \quad (2)$$

where $p_{i,xy}$ is the atomic shear stress p_{xy} for atom i.[17,27] Plugging Eq. (2) into Eq. (1), the microscopic expression of C^I_{44} can be simplified as[24]

$$C^I_{44} = -\frac{\bar{V}}{k_B T}\left\{\frac{1}{N}\sum_{i=1}^{N}\mathrm{var}(p_{i,xy}) + \frac{1}{N}\sum_{i=1}^{N}\left[\sum_{j\neq i}\mathrm{cov}(p_{i,xy},p_{j,xy})\right]\right\} = -\frac{\bar{V}}{k_B T}(X_1 + X_2) = -\frac{\bar{V}}{k_B T}X, \quad (3)$$

where $\mathrm{cov}(p_{i,xy},p_{j,xy})$ means the covariance of shear stresses between atom i and atom j. The density effect is separated out, in the average atomic volume ($\bar{V}$) term outside the brackets, such that the configurational dependence is completely represented by the terms inside the brackets (hereafter referred to as X). The X is the sum of two parts: $X_1 = \frac{1}{N}\Sigma_{i=1}^{N}\mathrm{var}(p_{i,xy})$ is the average variance of p_{xy} for each individual atom, and the second term, $X_2 = \frac{1}{N}\Sigma_{i=1}^{N}[\Sigma_{j\neq i}\mathrm{cov}(p_{i,xy},p_{j,xy})]$, is the average of total covariance, i.e., correlations, of p_{xy} for all atom pairs involving the center atom i.

To analyze the X, we first plot in Fig. 3 the distribution of the variance of p_{xy} in the samples. It is seen that for the MGs, the distribution is broad, showing that the variance of p_{xy} could be very different (changing from site to site) due to the different local environments in the amorphous structure. It is however narrow and sharp for the crystal, as all Cu (or Zr) atoms have the same local environment in B2 CuZr. Although the distribution spectra are different, the average values, X_1, are similar for all samples. This indicates that the covariance term, X_2, has to be responsible for the very different X. Specifically, X_2 (arrow in the inset of Fig. 3) is negative for the crystal, but positive for MGs (more so for faster cooling rates, rendering a decreasing G).

To find the origin of the different X_2, in Fig. 4 we plot the *average* covariance of p_{xy} for the atom pairs, as a function of the separation distance r_{ij}. We see that within $r_{ij} < 1.2$ nm, or in the short-to-medium range (SMR), the average correlation is strong, but it is much reduced (especially for MGs) for $r_{ij} > 1.2$ nm, or medium-to-long range (MLR). Note that this MLR correlation is rather weak but nonzero, and its total contribution to X_2 is significant because the number of atom pairs increases rapidly with the separation distance. Interest-

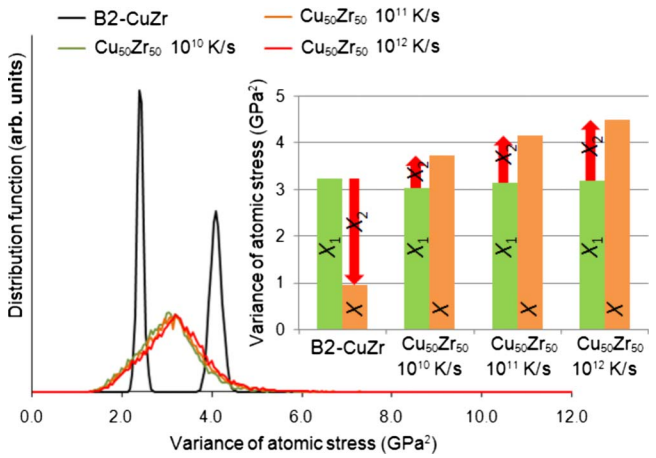

FIG. 3. (Color online) Distribution of the variance of p_{xy}. The peaks for MGs are broad, while the two sharp peaks for crystal correspond to Cu and Zr sites, respectively. Inset shows the X of the four samples (orange bars), which is the sum of the average variance of p_{xy} (X_1, green bars) and the covariance contribution (X_2, red arrows).

ingly, when evaluating these two contributing parts demarcated by a length scale of r_c=1.2 nm, which separates the strongly correlated SMR cluster and the vast MLR background/confinement, we observe that the total SMR contribution is positive and similar for all samples. In contrast, the total MLR contribution is negative, indicating that this is the region that, as a whole, responds to and couples with the inclusion SMR cluster. Since the overall SMR contribution to X_2 is not changing much and appears not very sensitive to configuration, especially for the MGs, the different X_2 (and hence G) in fact mainly originates from the different degree of MLR correlation of p_{xy}, see Fig. 5.

For MGs, fast cooling rate results in reduced MLR correlation, leading to a larger X_2 and X, and consequently a smaller G. In a crystal, however, MLR is rather strong so that X_2 and X are much reduced, enhancing the G. In any case, the degree of correlation (of p_{xy}) over MLR, or the transverse coupling between the atomic cluster and its confinement, is responsible for the G difference.

What is, then, the structural origin of the different MLR correlation of p_{xy}? A general answer is the varying degree of

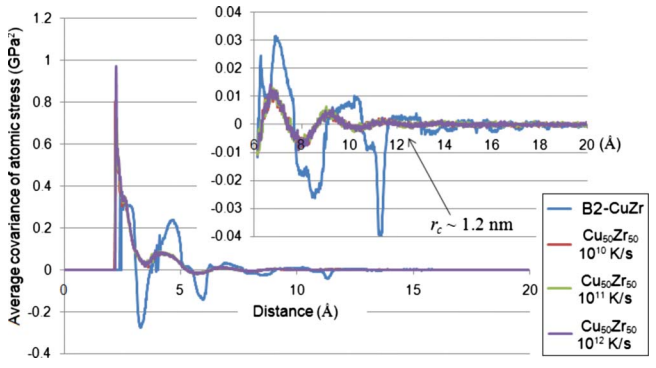

FIG. 4. (Color online) Average covariance of p_{xy} as a function of interatomic distance of the atom pair. Inset is a blowup of the tail.

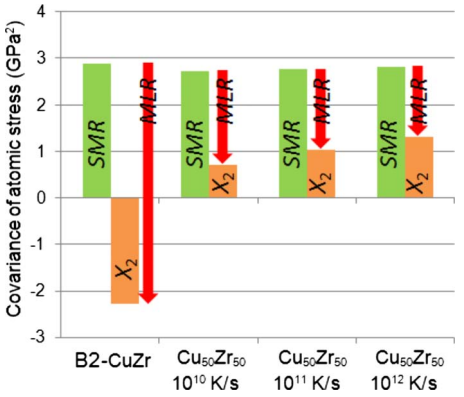

FIG. 5. (Color online) The covariance term X_2 (orange bars) decomposed into two parts: SMR contribution (green bars) and MLR contribution (red arrows).

ordering. To be specific, it is obvious that the crystal has long-range order while the glass does not. For the MGs, the controlling structural order is the locally preferred atomic clusters and their connection to form superclusters and/or network.[19,28] Our recent study has identified the full icosahedral cluster as the featured structural unit in the CuZr system, and they serve as the effective stabilizer against dynamic relaxation and shear transformation.[19–21] In particular, the full icosahedral network plays the role of an elastic backbone that controls yielding.[21] The network is thus the relatively rigid connection that strongly affects the MLR correlation of p_{xy}. Indeed, with higher cooling rate, the fraction and connectivity of full icosahedra in CuZr MGs decrease markedly,[19–21,29] significantly weakening the MLR correlation of p_{xy} and consequently lowering the G. It is interesting to note that this scenario is similar to the concept of rigidity percolation proposed by Thorpe for network glasses.[30] In fact, with lower fraction of the stable and rigid full icosahedra and consequently higher fraction of unstable "liquidlike" regions,[21,31] the sub-basin hopping in PEL becomes easier and more frequent, in the form of rearrangement of the un-

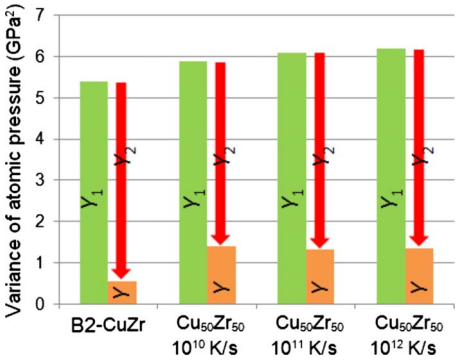

FIG. 6. (Color online) Variance of the atomic pressure (for bulk modulus), corresponding to Fig. 3. The histogram shows the Y term of the four samples (orange bars), which is the sum of the average variance of atomic pressure (Y_1, green bars) and the covariance contribution (Y_2, red arrows). Unlike the correlation of atomic shear stresses, now the correlation of atomic pressure is not very different in the four samples, and it is always negative, leading to a small Y (thus small B^I).

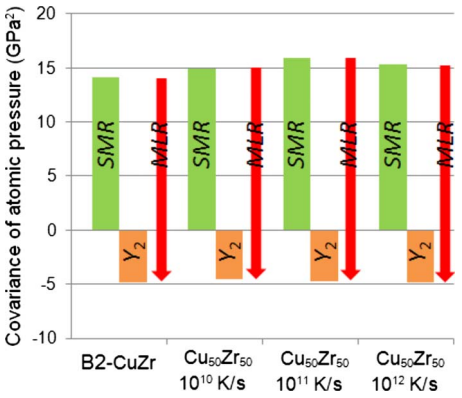

FIG. 7. (Color online) This figure corresponds to Fig. 4, but now for the bulk modulus. The covariance term Y_2 (orange bars) is decomposed into two parts: the SMR contribution (green bars) and the MLR contribution (red arrows). It is seen that the negative MLR correlation of atomic pressure is always strong and similar in all samples, crystalline or amorphous (prepared under different cooling rates).

stable atomic clusters. On the other hand, the controlling effect of different degree of ordering is also consistent with the results that the (configurational) entropic contribution dominates the different G: the more ordered, the lower the configurational entropy.

VI. BULK MODULUS AND THE POISSON'S RATIO

The above discussion of G^I (and G) focuses on the correlation of p_{xy}, i.e., the atomic *shear stress*. For B^I (and B), in contrast, the controlling microscopic quantity is the atomic *pressure* (p).[24]

$$P = \frac{1}{3V}\sum_{i=1}^{N}(m_i\vec{v}_i^2 + \vec{r}\cdot\vec{f}) = \frac{1}{N}\sum_{i=1}^{N}\frac{m_i\vec{v}_i^2 + \vec{r}\cdot\vec{f}}{3\bar{V}} = \frac{1}{N}\sum_{i=1}^{N}p_i, \tag{4}$$

$$\begin{aligned} B^I &= -\frac{V}{k_BT}\mathrm{var}(P) \\ &= -\frac{\bar{V}}{k_BT}\left\{\frac{1}{N}\sum_{i=1}^{N}\mathrm{var}(p_i) + \frac{1}{N}\sum_{i=1}^{N}\left[\sum_{j\neq i}\mathrm{cov}(p_i,p_j)\right]\right\} \\ &= -\frac{\bar{V}}{k_BT}(Y_1 + Y_2) = -\frac{\bar{V}}{k_BT}Y, \end{aligned} \tag{5}$$

where $Y_1 = \frac{1}{N}\Sigma_{i=1}^{N}\mathrm{var}(p_i)$, $Y_2 = \frac{1}{N}\Sigma_{i=1}^{N}[\Sigma_{j\neq i}\mathrm{cov}(p_i,p_j)]$.

To confirm that the B is not sensitive to configuration, we first list and compare the room-temperature (300 K) values of decomposed G and B in Table I. Since the cooling rate used to obtain MG samples in simulation (e.g., $\sim 10^{10}$ K/s) is much faster than in experiments (e.g., ~ 1 K/s), and the G is sensitive to the degree of structural ordering and the details of atomic configuration (which are sensitive to the cooling rate), it is expected that the G values of simulated MGs are noticeably smaller than typical experimental values. While for B, which is insensitive to structural details and cooling rate, the values of simulated MGs are close to those measured in experiments. As a result, G/B ratio (ν) of simulated MGs is smaller (larger) than we usually have in experiments.[31] Calculated modulus of the crystal does not have such a cooling rate effect.

For B^I, we can also plot figures (Figs. 6 and 7) similar to those in the inset of Fig. 3 and in Fig. 5. Here for the bulk modulus the controlling factor is the correlation of atomic pressure (p), instead of the correlation of atomic shear stress (p_{xy}) as for the case of shear modulus. Unlike for p_{xy}, the MLR correlation of p remains strong and similar in all samples, thus the variations in structural ordering do not drastically change B. In other words, the compressibility is not sensitive to the subtle structural details (e.g., ordering, symmetry) as shear resistance is, as long as the density, average coordination number and bond lengths/types are generally similar. In the PEL, correspondingly, the local profile along the dimension of volumetric strain is not configurational sensitive as shown in Fig. 2. The different effect of structural order on the correlation of p_{xy} and p is also consistent with the behavior of long-wavelength acoustic phonons: the transverse phonon is much softened in MGs, while the longitudinal phonon is less affected.[32]

VII. CONCLUDING REMARKS

In summary, quantitative insight regarding the behavior of G versus B is gained from atomistic simulations of MGs (and the crystal counterpart), with special focus on the comparison between MGs with different cooling history. The configurational dependence of G is a demonstration of the rugged PEL in MGs, and dominated by the entropic contribution in the free energy. Microscopically, it is the large variation in the MLR correlation of atomic shear stress that is responsible for the strong configurational dependence of G. The degree and extent of structural ordering is the microscopic origin of

TABLE I. Decomposed shear modulus and bulk modulus of the four samples at 300 K (unit for modulus is GPa). Note that G^I (and G) is very sensitive to configuration, while B^I (and B) is not. Consequently, the G/B ratio (or Poisson's ratio, ν) is a dimensionless indicator of the internal atomic configuration, or the degree of structural ordering (Ref. 31).

		G^I	G^{II}	G^{III}	G	B^I	B^{II}	B^{III}	B	G/B	ν
Crystal		−2.92	0.75	36.2	34.02	−2.32	0.31	120.3	118.3	0.288	0.369
Glass	10^{10} K/s	−16.03	0.93	34.55	19.45	−6.00	0.31	112.5	106.8	0.182	0.414
	10^{11} K/s	−17.89	0.93	34.49	17.53	−5.67	0.31	112.4	107.1	0.164	0.422
	10^{12} K/s	−19.41	0.93	34.49	16.01	−5.75	0.31	112.3	106.9	0.150	0.429

the different levels of correlations. Reduced order leads to considerably weaker MLR transverse correlation and hence obviously lower G, but does not affect much the atomic pressure correlations underlying B, rendering an insensitive configurational dependence of B.

The authors thank H.W. Sheng for the EAM potentials, and M. L. Falk, R. C. Cammarata, and M. Widom for valuable suggestions. This work was supported by U.S.-DoE-BES, Division of Materials Sciences and Engineering, under Contract No. DE-FG02-09ER46056.

*cheng@jhu.edu
†ema@jhu.edu

[1] A. L. Greer and E. Ma, MRS Bull. **32**, 611 (2007).
[2] C. A. Schuh, T. C. Hufnagel, and U. Ramamurty, Acta Mater. **55**, 4067 (2007).
[3] M. L. Lind, G. Duan, and W. L. Johnson, Phys. Rev. Lett. **97**, 015501 (2006).
[4] G. Duan, M. L. Lind, M. D. Demetriou, W. L. Johnson, W. A. Goddard III, T. Çağin, and K. Sawmer, Appl. Phys. Lett. **89**, 151901 (2006).
[5] J. Hachenberg, D. Bedorf, K. Samwer, R. Richert, A. Kahl, M. D. Demetriou, and W. L. Johnson, Appl. Phys. Lett. **92**, 131911 (2008).
[6] K. W. Park, C. M. Lee, M. Wakeda, Y. Shibutani, M. L. Falk, and J. C. Lee, Acta Mater. **56**, 5440 (2008).
[7] W. L. Johnson and K. Samwer, Phys. Rev. Lett. **95**, 195501 (2005).
[8] M. D. Demetriou, J. S. Harmon, M. Tao, G. Duan, K. Samwer, and W. L. Johnson, Phys. Rev. Lett. **97**, 065502 (2006).
[9] W. L. Johnson, M. D. Demetriou, J. S. Harmon, M. L. Lind, and K. Samwer, MRS Bull. **32**, 644 (2007).
[10] A. V. Granato, Phys. Rev. Lett. **68**, 974 (1992).
[11] A. V. Granato, J. Non-Cryst. Solids **307-310**, 376 (2002).
[12] S. V. Khonik, A. V. Granato, D. M. Joncich, A. Pompe, and V. A. Khonik, Phys. Rev. Lett. **100**, 065501 (2008).
[13] D. J. Safarik and R. B. Schwarz, Acta Mater. **55**, 5736 (2007).
[14] D. Weaire, M. F. Ashby, J. Logan, and M. J. Weins, Acta Metall. **19**, 779 (1971).
[15] G. Knuyt, L. DeSchepper, and L. M. Stals, J. Phys. F: Met. Phys. **16**, 1989 (1986).
[16] C. Maloney and A. Lemaître, Phys. Rev. Lett. **93**, 195501 (2004).
[17] T. Egami, K. Maeda, and V. Vitek, Philos. Mag. A **41**, 883 (1980).
[18] S. J. Plimpton, J. Comput. Phys. **117**, 1 (1995).
[19] Y. Q. Cheng, E. Ma, and H. W. Sheng, Phys. Rev. Lett. **102**, 245501 (2009).
[20] Y. Q. Cheng, H. W. Sheng, and E. Ma, Phys. Rev. B **78**, 014207 (2008).
[21] Y. Q. Cheng, A. J. Cao, H. W. Sheng, and E. Ma, Acta Mater. **56**, 5263 (2008).
[22] In experiments B2 CuZr is not stable at low temperatures, but this metastable phase can be easily retained and studied in simulations at room temperature.
[23] T. Çağin and J. R. Ray, Phys. Rev. B **38**, 7940 (1988).
[24] See EPAPS Document No. E-PRBMDO-80-010930. For more information on EPAPS, see http://www.aip.org/pubservs/epaps.html.
[25] F. H. Stillinger, Science **267**, 1935 (1995).
[26] J. S. Harmon, M. D. Demetriou, W. L. Johnson, and K. Samwer, Phys. Rev. Lett. **99**, 135502 (2007).
[27] We use an average atomic volume without differentiating different atom species because we only study the stress distribution, correlation, and comparison for different samples. We are not solving the values of the atomic stresses, which require a definition of "atomic volume" for each specific atom.
[28] C. P. Royall, S. R. Williams, T. Ohtsuka, and H. Tanaka, Nature Mater. **7**, 556 (2008).
[29] Y. Q. Cheng and E. Ma, Appl. Phys. Lett. **93**, 051910 (2008).
[30] M. F. Thorpe, J. Non-Cryst. Solids **57**, 355 (1983).
[31] Y. Q. Cheng, A. J. Cao, and E. Ma, Acta Mater. **57**, 3253 (2009).
[32] B. Golding, B. G. Bagley, and F. S. L. Hsu, Phys. Rev. Lett. **29**, 68 (1972).